THE ASTROPHYSICAL JOURNAL, 553:1036–1041, 2001 June 1

INTERFEROMETRIC PHASE CORRECTION USING 183 GHz WATER VAPOR MONITORS

MARTINA C. WIEDNER[1] AND RICHARD E. HILLS
Mullard Radio Astronomy Observatory, Cavendish Laboratory, Madingley Road, Cambridge, CB3 0HE, UK; mwiedner@cfa.harvard.edu, richard@mrao.cam.ac.uk
JOHN E. CARLSTROM
Department of Astronomy and Astrophysics, University of Chicago, Chicago, IL 60637; jc@hyde.uchicago.edu
AND
OLIVER P. LAY
Jet Propulsion Laboratory, California Institute of Technology, Pasadena, CA 91109; oplay@mail1.jpl.nasa.gov
Received 2000 April 28; accepted 2000 December 22

ABSTRACT

The angular resolution that can be obtained by ground-based aperture synthesis telescopes at millimeter and submillimeter wavelengths is limited by phase fluctuations caused by water vapor in the Earth's atmosphere. We describe here the successful correction of such fluctuations during observations at 0.85 mm wavelength with an interferometer consisting of the James Clark Maxwell Telescope and the Caltech Submillimeter Observatory. This was achieved by using two 183 GHz heterodyne radiometers to measure the water vapor content along the line of sight of each telescope. Further development of such techniques will enable future telescopes, such as the Submillimeter Array and the Atacama Large Millimeter Array, to reach their full capability, providing a resolution of up to 0.″01.

Subject headings: atmospheric effects — instrumentation: adaptive optics — site testing — techniques: interferometric

1. INTRODUCTION

Absorption by atmospheric water vapor is a major constraint on observations in the millimeter and far-IR wave bands. It is possible, however, to make observations down to about 0.3 mm wavelength (~900 GHz) by working at sufficiently high, dry sites such as Mauna Kea on Hawaii, the South Pole, or Chajnantor in Chile, the site chosen for the Atacama Large Millimeter Array (ALMA). The high refractive index of water vapor at these wavelengths, together with its variable abundance in the atmosphere, also gives rise to distortions of the wave front (Hinder & Ryle 1971)—very similar to "seeing." (At optical wavelengths the fluctuations are caused by temperature gradients, and the scales of the atmospheric structures involved are much smaller.) If uncorrected, these distortions limit the angular resolution that can be obtained from even the best sites to a few tenths of an arcsecond.

Here we describe the first use of radiometers monitoring the 183 GHz rotational transition of water vapor to correct for these effects. The two radiometers were built at the Mullard Radio Astronomy Observatory (MRAO) in Cambridge, UK, and installed on the James Clerk Maxwell Telescope (JCMT) and the Caltech Submillimeter Observatory (CSO) on Mauna Kea, Hawaii. These two telescopes can be linked together to operate as an interferometer with a baseline of 164 m (Carlstrom et al. 1994; Lay et al. 1998). The radiometers measure the amounts of atmospheric water vapor above the telescopes to high accuracy, so that the varying propagation delay can be estimated and a correction applied to the phase of the astronomical signal.

1.1. *Cause of Phase Fluctuations*

The phase measured by an interferometer is a measure of the difference in the arrival times of the signals at the two antennas, as shown in Figure 1. The phase difference contains information about the location and structure of the source but is also affected by water vapor in the atmosphere. Moist air has a higher refractive index than dry air, and therefore electromagnetic waves propagate more slowly through a wet atmosphere. If there is more water vapor along the electrical path of, e.g., telescope 1, the radiation to telescope 1 will experience an additional delay and the measured phase will increase by $\Delta\phi$. With wind, the amount of water vapor in the beam of each telescope will change over time and so will the detected phase. As a result, the source appears to move in the sky, and, if the signals are integrated over a period of time that is long compared with the time scale of the fluctuations (a few to tens of seconds), resolution as well as signal strength will be degraded. In average nighttime conditions on Mauna Kea, the Fried length (r_0) is 580 m at 1 mm wavelength, i.e., the effective resolution of long exposures through the atmosphere is the same as the resolution obtained with a telescope of 580 m diameter (Fried 1965). Very good descriptions of radio seeing are given in, e.g., Masson (1994), Thompson, Moran, & Swenson (1994), and Carilli & Holdaway (1999).

1.2. *Phase Correction Methods*

There is an extensive literature on phase correction at radio wavelengths; an incomplete list of articles includes Westwater (1967); Schaper, Staelin, & Waters (1970); Holdaway (1992); Sutton & Hueckstaedt (1996); Lay (1997a, 1997b). Basically there are two different methods.

1. The phase offset due to the atmosphere can be measured *directly* by observing a calibrator, i.e., a strong point source whose position and hence theoretical phase are well known. Assuming phase fluctuations due to instrumental effects are small, the difference between the measured and the theoretical phase gives the phase offset introduced by the atmosphere. The phase offsets, which are interpolated between measurements on the calibrator, are subtracted

[1] Current address: Harvard-Smithsonian Center for Astrophysics, 60 Garden Street, Cambridge, MA 02138.

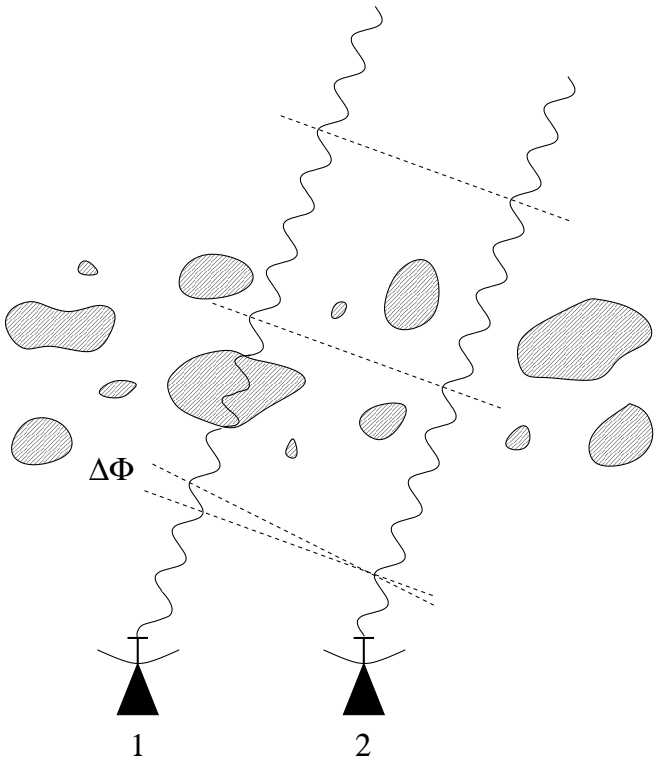

FIG. 1.—How atmospheric water vapor causes phase shifts in millimeter and submillimeter interferometry. The two sinusoidal lines symbolize an electromagnetic wave from an astronomical object to two elements of an interferometer. The wave front (*dashed line*) is perpendicular to the direction from the source. If there is water vapor (*hatched areas*) along the line of sight to one telescope (*object 1*) this wave is retarded. The inclination of the wave front is changed by an angle $\Delta\phi$, which is detected by the interferometer as a phase shift from the undisturbed phase.

from the measured phase of an astronomical source. This method can be further subdivided into (*a*) *fast switching* (Holdaway & Owen 1995; Morita et al. 2000), where the calibration cycle is shorter than the timescale of the atmospheric fluctuations, (*b*) *beam switching*, where the secondary rather than the primary mirror is moved, and (*c*) *the subarray method* (Asaki et al. 1996), where one subarray is continuously monitoring the calibrator while the other is observing the source.

2. The correction can be determined *indirectly* by detecting the emission from water molecules and calculating the phase error from the differences in the amounts of water vapor along the paths to the individual antennas. Water vapor emits several spectral lines, e.g., at 22, 183, and 325 GHz, as well as a "continuum." (This "continuum" actually consists of the wings of very strong water vapor lines in the infrared and other contributions; for more detail see, e.g., Rosenkranz 1998.) There are two different approaches to determine the amount of water vapor: (*a*) *total power method* (Welch 1994; Bremer 1995; Bower et al. 1997), where the astronomical receivers measure the continuum emission, and (*b*) *radiometric phase correction*, where the emission from a water vapor line is measured by dedicated instruments. So far, radiometers have been built or are under construction to monitor the 22 GHz line (Very Large Baseline Interferometry, Elgered et al. 1991; Meteorology, Westwater & Guiraud 1980; Very Large Array, Resch, Hogg, & Napier 1984; Butler 1999; Owens Valley Radio Observatory, Marvel & Woody 1998; Woody, Carpenter, & Scoville 2000) and the 183 GHz line (CSO-JCMT, Wiedner 1998; Atacama Large Millimeter Array, Delgado et al. 1999; Hills & Richer 2000).

Which phase correction technique is most effective will depend on the interferometer, in particular on the stability of its receivers, but also on the slew speed of the antennas and other parameters, as well as on the weather at the site in question.

1.3. *Atmospheric Emission on Mauna Kea*

The top panel of Figure 2 shows the atmospheric emission on Mauna Kea for typical values of precipitable water vapor (PWV). (1 mm PWV is the amount of water vapor that would yield a column of 1 mm if it were condensed out of the atmosphere.) The 22 GHz line is always optically thin, whereas the line at 183 GHz starts saturating at the center (but not in the line wings) with only 2 mm PWV.

An increase in the amount of PWV by 0.16 mm is approximately equivalent to lengthening the electromagnetic wave's electrical path by an additional 1 mm (Sutton & Hueckstaedt 1996). The sensitivity, plotted in the bottom panel of Figure 2, indicates by how many kelvins the sky emission will change per millimeter of additional electrical path. The sensitivity is a function of frequency as well as amount, temperature, and pressure of the PWV. For a given amount of underlying water vapor, the maximum sensitivity is reached at those frequencies where the optical depth

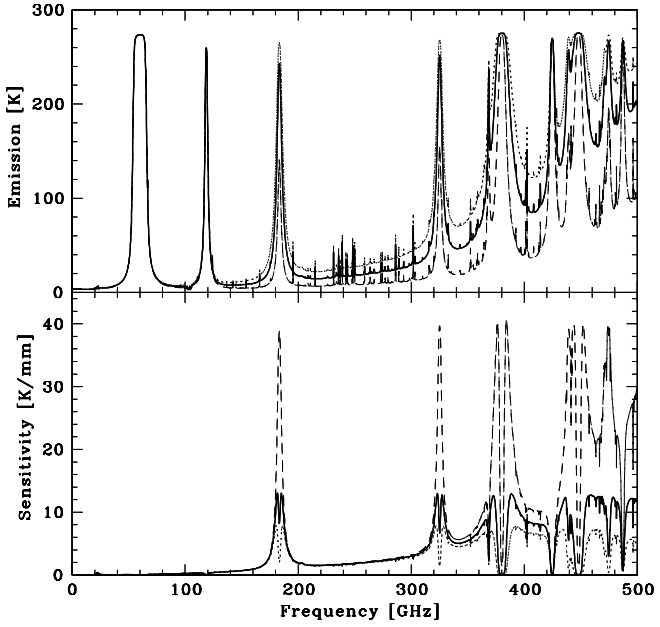

FIG. 2.—Atmospheric emission and sensitivity to electrical path length changes on Mauna Kea. Values are calculated using the atmospheric transmission model (ATM; Pardo 1996) with an exponential distribution of water vapor and a scale height of 2 km. Different distributions of water vapor, as well as different temperatures and pressures, would change the line profiles. *Top:* The atmospheric emission plotted as a function of frequency for the minimum of 0.4 mm PWV (*dashed line*), the 25% quartile of 1.2 mm PWV (*solid line*), and the 50% quartile of 2.0 mm PWV (*dotted line*). There are water vapor lines at 22 (only a few Kelvin), 183, 321, 325, 380, 390, several lines around 440, 470, 474, and 488 GHz. The lines around 60 GHz and at 119 GHz are due to oxygen. *Bottom:* The sensitivity, which is defined as the change in sky brightness temperature for the amount of PWV that will add 1 mm to the electrical path length, is plotted for the same amounts of PWV (*same line styles*).

is ~ 1. This maximum has a value of $\sim 16/w$ in units of kelvins per millimeter of electrical-path length, where w is the amount of PWV in millimeters. The strength of the 183 GHz line is such that this maximum sensitivity is always achieved at some suitably chosen frequency in the line center or wings, even under very dry conditions of ~ 0.5 mm PWV. The sensitivity of the 22 GHz line (~ 0.4 K mm^{-1}) is, by contrast, very much lower at dry sites, ~ 33 times lower than the 183 GHz line for 1.2 mm PWV and ~ 100 times lower for 0.4 mm PWV.

2. THE 183 GHz WATER VAPOR MONITOR

2.1. *Advantages of* 183 GHz *Radiometers*

Receivers at 22 GHz typically have lower noise temperatures than those at 183 GHz, but on dry sites the 183 GHz monitors will be able to measure the electrical path with higher accuracy because of the much higher conversion factor from sky brightness temperature in kelvins to electrical-path length in millimeters. This means that a simple, uncooled 183 GHz system can provide satisfactory phase correction at up to at least 350 GHz, whereas a 22 GHz system would need to be cooled. Another advantage of monitoring the strong 183 GHz line is that ground pick-up is comparatively weak and introduces a much smaller error in the predicted electrical path. Feed optics for 183 GHz are also much smaller than for 22 GHz, and the radiometer beam is more similar to the telescope beam for millimeter and submillimeter wavelength observations. Good sensitivity can also be obtained at frequencies higher than 183 GHz, but it is more difficult to build suitable receivers. The astronomical receivers could also be used for phase correction (total power method, method 2*a* in § 1.2), either if their gain fluctuations are smaller than $\sim 10^{-4}$ or if the receivers are frequently calibrated so that their gain variations are known to this accuracy. Frequent (~ 1 Hz) calibration of an astronomical receiver would, however, reduce the observing time considerably.

2.2. *Selected Frequency Channels*

Figure 3 shows the water vapor line at 183 GHz for the minimum amount of precipitable water vapor as well as the 25%, 50%, and 75% nighttime quartiles of PWV for Mauna Kea. (The 25% quartile of 1.2 mm PWV indicates that during 25% of the nights the amount of PWV is equal to or less than 1.2 mm.) Because the line center starts saturating above 2 mm PWV, the radiometers measure the line intensity in three double-sideband channels 1.0–1.4, 3.7–4.7, and 7.3–8.3 GHz away from the line center.

2.3. *Optics and Calibration*

Water vapor monitors (WVM) are installed on both the CSO and JCMT. The atmospheric emission is collected by the telescope's primary mirror, reflected from the secondary, and then directed to the water vapor monitors by a small (about 0.2×0.1 m) pick-off mirror mounted offset ($\sim 7'$ at JCMT, $\sim 12'$ at CSO on the sky) from the astronomical beam above each telescope's tertiary mirror. In addition, the radiometer beam diverges by $\sim 3'$ at the JCMT and by $\sim 5'$ at the CSO. At 1 km the WVM beam from the JCMT is offset from the astronomical beam by 2.1 m and has a diameter of 16.6 m compared with the 15 m JCMT beam; at the CSO the WVM beam is offset by 3.4 m and has a diameter of 13.5 m compared with the 10.4 m CSO beam.

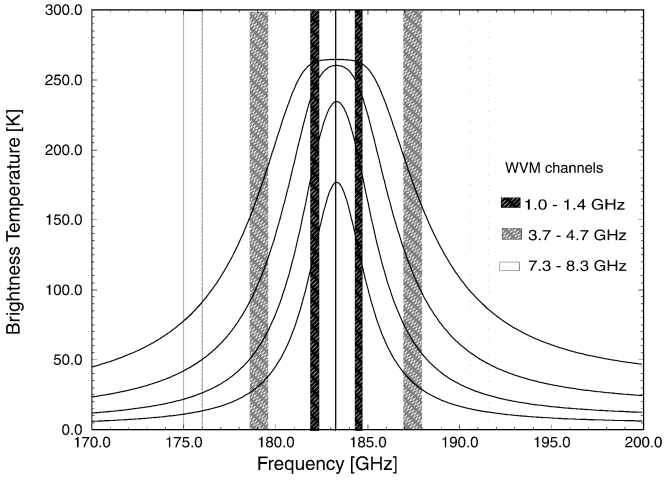

FIG. 3.—Frequency channels of the water vapor monitors superposed on the 183 GHz line. The four curves show the profile of the 183 GHz water vapor line for 0.5, 1, 2, and 4 mm PWV. The water vapor monitor measures the intensity of the line in three twice–double-sided frequency bands: 1.0–1.4 (*black*), 3.7–4.7 (*dark gray*), and 7.3–8.3 GHz (*light gray*) away from the line center.

At the heights where most of the PWV is expected the radiometer and astronomical beams overlap very well.

For calibration, a hot (100° C) and a warm load (30° C) are located inside the $\sim 0.6 \times 0.5 \times 0.4$ m box of the water vapor monitor. A "flip mirror" selects between radiation from the sky or from one of the calibration loads. In the normal calibration cycle of 1 s the radiometer integrates 400 ms on the sky and 200 ms on each load. The flip mirror is moving during the remaining 200 ms.

2.4. *Electronics*

The atmospheric radiation is collected by a corrugated feed horn and mixed with a local oscillator (LO) signal at 91.655 GHz (exactly half the frequency of the water vapor line) in a subharmonically pumped double-sideband Schottky mixer. The WVM contains a phase lock loop that keeps the frequency of the LO constant, and all electronics is temperature-regulated to stabilize the LO's power level and the amplifiers' gains. The 0.5–8.5 GHz intermediate frequency (IF) is amplified and then split into three channels. Each is mixed down a second time with local oscillators at 1.2, 4.2, and 7.8 GHz, respectively. This ensures a greater accuracy in the center frequency of each channel than a bandpass filter would yield. The resulting IF signals are passed through low-pass filters of 200, 500, and 500 MHz width, respectively, and detected.

The detected voltages are converted into a pulse train by voltage-to-frequency converters and sent to a counter card on an industrial PC. The control computer at the JCMT synchronizes the integration times of the water vapor monitors on the two telescopes, records the frequencies, and converts them into apparent sky brightness.

The instrument is temperature-regulated but uses uncooled mixers, resulting in system temperatures between 1800 and 2700 K. Allan variance calculations show that the measurements are dominated by thermal noise for integration times shorter than a few seconds, when gain fluctuations start becoming significant. This emphasizes the need for frequent calibration.

Assuming a conversion factor of 5.0 K mm^{-1} of electrical path (for channel 2 at 2 mm PWV) and no other uncertainties or systematic errors, the best path correction would result in an rms of ~ 25 μm.

2.5. *Data Reduction*

To obtain all the data presented hereafter, the CSO-JCMT interferometer observed bright point sources with the shortest possible integration time of 10 s. After Doppler tracking, any deviations from a constant phase are due to the atmosphere or to instrumental noise.

Prior to the observation the brightness temperature of the water vapor monitors is calibrated with an ambient absorber and an absorber dipped in liquid nitrogen. The beam efficiency (coupling) is calculated from a sky dip.

The water vapor monitors are synchronized and take data every second, integrating 0.4 s on the sky and 0.2 s on each calibration load, returning three measurements for each of the three channels every second. The measurements from the hot and warm loads are smoothed and used to convert the readings from the sky into brightness temperatures. For each channel a separate conversion factor is chosen (see below) to provide three independent estimates of the phase correction.

For each channel all WVM measurements corresponding to one 10 s interferometer integration are averaged and subtracted from the interferometer phase measurement. Because the absolute phase is arbitrary, a constant phase offset is subtracted from all data. Before the rms phase is calculated, a line is fitted to the data and subtracted, because a linear phase gradient over several minutes is unlikely to be due to water vapor but is most probably introduced by the CSO-JCMT interferometer, e.g., drifts in the LO phase or imperfect determination of the baseline.

The conversion factor depends on the frequencies of the WVM channel and the frequency of the interferometer observations, as well as on the amount, temperature, and pressure of the PWV. The frequencies are well known. Assuming an exponential distribution of PWV with a scale height of 2 km, a ground temperature of 275 K, and a ground pressure of 625 mbar, the amount of PWV can be computed from each channel. Usually the results derived from each channel individually agree within 10%. Using the same models, the theoretical conversion factor can be determined. For bright point sources, where the phase is not dominated by noise, an optimal conversion factor can be found by minimizing the rms of the corrected phase. Table 1 gives an example of the theoretical and optimal conversion factor for each channel and the phase correction that can be achieved with them. Though the theoretical and the optimal conversion factors may differ by up to $\sim 35\%$, the phase correction achieved with them are of the same quality within statistical errors. Because the line shape contains information about the temperature and pressure of the PWV (as well as other atmospheric components such as liquid water), it could in principle be used to modify the atmospheric model that calculates the theoretical conversion factor. Currently, however, the accuracy of our brightness temperature measurements does not seem sufficient, but other radiometers with many (~ 32) channels are expected to retrieve this information (Staguhn et al. 1998).

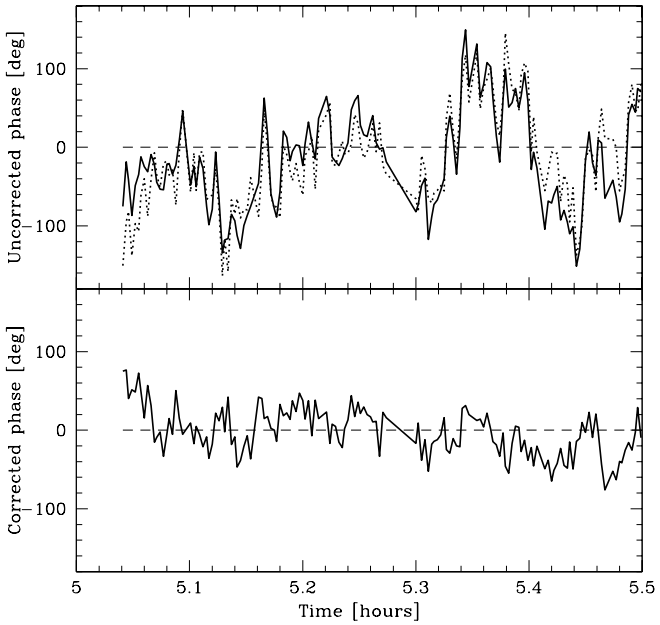

FIG. 4.—Phase corrections obtained in 1998 October at the CSO-JCMT interferometer with a baseline of 164 m for average atmospheric conditions of 2.6 mm PWV along the line of sight. *Top:* The solid line represents the interferometric phase measured at 354 GHz after Doppler correction; the dotted line shows the predicted phase corrections using the 183 GHz WVMs. *Bottom:* After correction the phase fluctuations are reduced from 60° to 26° rms, corresponding to a reduction in electrical path errors from 141 to 61 μm.

2.6. *Results*

Figure 4 shows typical phase correction results in normal nighttime weather on Mauna Kea, when the CSO tau meter measured an atmospheric transmission of $1-e^{0.11}$ at 225 GHz ($\tau_{225} = 0.11$). The CSO-JCMT interferometer observed bright hydrogen recombination line maser emission toward MWC 349 at 354 GHz. The solid curve in the

TABLE 1

DEPENDENCE OF PHASE CORRECTION ON CONVERSION FACTOR

	CHANNEL 1			CHANNEL 2			CHANNEL 3		
METHOD	Conversion Factor (K rad^{-1})	rms (deg)	rms (μm)	Conversion Factor (K rad^{-1})	rms (deg)	rms (μm)	Conversion Factor (K rad^{-1})	rms (deg)	rms (μm)
Theory.....	0.27	41	97	0.70	27	64	0.41	41	97
Optimal.....	0.37	38	89	0.62	26	61	0.49	40	94

NOTES.—Using one data set as an example, the theoretical conversion factor for each of the three WVM channels is calculated as described in § 2.5 and with it the interferometer phase is corrected, reducing the rms phase from 60° (142 μm) to the listed value. The second line lists the optimal conversion factor for each channel, obtained by minimizing the rms of the residual phase. Though the optimal conversion factors differ from the theoretical factors by around 20%, the correction using the theoretical values is only very little worse than the best correction.

TABLE 2

RESULTS OF PHASE CORRECTIONS USING 183 GHz WVMs

Date (1)	Uncorrected Phase (deg) (2)	Corrected Phase (deg) (3)	Uncorrected Phase (μm) (4)	Corrected Phase (μm) (5)	Duration (minutes) (6)	τ_{225} (7)	PWV Along Line of Sight (mm) (8)	Conversion Factor (K rad^{-1}) (9)	Comments (10)
1996 Nov 29.....	55	23	131	55	30	0.062	2.0	0.64	...
1997 May	...	...	...	...	...	...	...	...	No correlation
1997 Nov 9	Random	48	290	113	12	0.17	4.3	0.60	...
	Random	38	290	90	12	0.17	4.3	0.60	Same as above, but spikes removed
	79	47	186	111	6	0.17	4.3	0.60	...
	103	55	243	130	6	0.17	4.3	0.60	...
	110	60	259	141	6	0.17	4.3	0.60	...
1998 Oct 25	60	26	141	61	30	0.11	2.6	0.62	See Fig. 4
	51	26	120	61	30	0.11	2.7	0.62	...
	31	19	73	45	18	0.11	2.9	0.75	...
	27	18	64	42	24	0.11	3.0	0.75	...
1998 Oct 23	33	35	78	82	30	0.17	4.8	0.45	Phase stable, but high PWV

NOTES.—The table lists all 183 GHz phase corrections for time periods longer than 5 minutes. The date of the measurement is listed in Col. (1). Cols. (2)–(5) contain the rms of the uncorrected phase and of the phase corrected with the optimal conversion factor listed in Col. (9). The time over which this rms is calculated is noted in Col. (6). The CSO τ-meter reading is listed in Col. (7) and the PWV along the line of sight estimated from PWV $= 25(\tau_{225}-0.013)/\sin(\text{elevation})$ is noted in Col. (8). (The formula was derived using the ATM model; Pardo 1996.) The last column contains comments.

top panel displays the *measured* phase after Doppler correction, integrated over 10 s. It represents the atmospheric phase fluctuations and some electronic phase noise. The dashed line shows the phase *predicted* by channel 2 of the WVMs averaged over the same time. The measured and predicted phases agree well, and phase correction reduces the rms phase fluctuations from 60° (141 μm) to 26° (61 μm) over 30 minutes. If one would integrate on source for 30 minutes, 50% of the astronomical flux would be lost because of decorrelation, but with phase correction the loss would amount to only 10%. Phase corrections using channels 1 and 3 (see Table 1) give poorer results.

All reduced test data from the CSO-JCMT interferometer of at least 5 minutes duration are summarized in Table 2. In all cases the best correction, which is listed in the table, was achieved by using channel 2 alone, because for 2–6 mm PWV channel 2 has the highest conversion factor and therefore the lowest noise compared to the brightness-temperature fluctuations due to water vapor. Corrections with weighted averages of all three channels do not reduce the rms. During 1997 May no correlation was found, most probably because the computer clocks were unsynchronized. In all other cases the water vapor monitors reduce the rms phase, except during one very wet ($\tau_{225} = 0.17$) but stable (0.″3 radio seeing) night when the correction adds a little noise to the data. In bad weather (4.3 mm PWV along the line of sight), radiometer phase correction at 354 GHz reduces the rms phase on 12 minute observations from essentially random (300 μm) to 38° (90 μm).

Ideally the corrected phase should be constant. The residual fluctuations can have many origins. Instrumental noise from the WVM is estimated to contribute at least 25 μm. There might be instrumental phase noise from the interferometer, which is expected to be less than 28 μm. The data reduction process, e.g., inaccurately determined beam efficiency, might also contribute to the residual phase. Other constituents of the atmosphere, such as liquid water, might contribute to the brightness-temperature fluctuations but not affect the electrical path, or they might affect it in a different way.

3. CONCLUSIONS

Two radiometers measuring the emission from the 183 GHz water vapor line have been built and tests have been performed which demonstrate that our system can substantially improve the interferometer data. Though more testing is necessary, the reported results suggest that this method promises to considerably reduce phase fluctuations of millimeter and submillimeter interferometers located at dry sites, such as the Submillimeter Array (SMA) or the Atacama Large Millimeter Array (ALMA).

We would like to thank all the technicians, in particular J. E. Jennings from MRAO, who helped build the water vapor monitors, as well as the CSO-JCMT interferometry team, who played an essential role in the testing. We are grateful for many discussions with T. K. Sridharan and other colleagues at the CfA, as well as for very helpful comments by the referee J. Staguhn. M. C. W. was supported by an HSP III scholar-ship of the German Academic Exchange service as well as the Sir Isaac Newton Scholarship.

The JCMT is operated by the Royal Observatories on behalf of the Particle Physics and Astronomy Research Council of the United Kingdom, the Netherlands Organization for Scientific Research, and the National Research Council of Canada. Research at the CSO is supported by NSF grant AST 96-15025.

REFERENCES

Asaki, Y., Saito, M., Kawabe, R., Morita, K.-I., Sasao, T. 1996, Radio Sci., 31, 1615
Bower, G. C., Backer, D. C., Plambeck, R. L., & Wright, M. C. H. 1997, J. Geophys. Res., 102, 16773
Bremer, M. 1995, The Phase Project: Observations on Quasars, IRAM Technical Report 238
Butler, B. 1999, VLA Scientific Memo 177 (NRAO)
Carilli, C. L., & Holdaway, M. A. 1999, MMA Memo 262 (NRAO)
Carlstrom, J. E., Hills, R. E., Lay, O. P., Force, B., Hall, C. G., Phillips, T. G., & Schinckel, A. E. 1994, in ASP Conf. Ser. 59, Astronomy with Millimeter and Submillimeter Wave Interferometry, ed. M. Ishiguro & W. J. Welch (San Francisco: ASP), 35
Delgado, G., Otàrola, A., Belitsky, V., & Urbain, D. 1999, MMA Memo 271 (NRAO)
Elgered, G., Davis, J. L., Herring, T. A., & Shapiro, I. I. 1991, J. Geophys. Res., 96, 6541
Fried, D. L. 1965, J. Opt. Soc. Am., 55, 1427
Hills, R. E., & Richer, J. S. 2000, ALMA Memo 303 (NRAO)
Hinder, R., & Ryle, M. 1971, MNRAS, 154, 229
Holdaway, M. A. 1992, MMA Memo 84 (NRAO)
Holdaway, M. A., & Owen, F. N. 1995, MMA Memo 126 (NRAO)
Lay, O. P. 1997a, A&AS, 122, 535
———. 1997b, A&AS, 122, 547
Lay, O. P., Wiedner, M. C., Carlstrom, J. E., & Hills, R. E. 1998, Proc. SPIE, 3357, 254
Marvel, K. B., & Woody, D. P. 1998, Proc. SPIE, 3357, 442
Masson, C. R. 1994, in IAU Symp. 158, Very High Angular Resolution Imaging, ed. J. G. Robertson & W. J. Tango (Dordrecht: Kluwer), 1
Morita, K.-I., et al. 2000, in ASP Conf. Ser. 217, Imaging at Radio through Submillimeter Wavelengths, ed. J. G. Mangum & S. J. E. Radford (San Francisco: ASP), 340
Pardo, J. R., 1996, Ph.D. thesis, Univ. Pierre et Marie Curie–Univ. Complutense de Madrid
Resch, G. M., Hogg, D. E., & Napier, P. J. 1984, Radio Sci., 19, 411
Rosenkranz, P. W. 1998, Radio Sci., 33, 919
Schaper, L. W., Staelin, D. H., & Waters, J. W. 1970, Proc. IEEE, 58, 272
Staguhn, J., Harris, A. I., Plambeck, R. L., & Welch, W. J. 1998, Proc. SPIE, 3357, 432
Sutton, E. C., & Hueckstaedt, R. M., 1996, A&AS, 119, 559
Thompson, A. R., Moran, J. M., & Swenson, G. W. 1994, Interferometry and Synthesis in Radio Astronomy (Malabar: Krieger)
Welch, W. J. 1994, in ASP Conf. Ser. 59, Astronomy with Millimeter and Submillimeter Wave Interferometry, ed. M. Ishiguro & W. J. Welch (San Francisco: ASP), 1
Westwater, E. R. 1967, ESSA Technical Report IER 30-ITSA 30
Westwater, E. R., & Guiraud, F. O. 1980, Radio Sci., 15, 947
Wiedner, M. C. 1998, Ph.D. thesis, Cambridge Univ. (http://cfa-www.harvard.edu/mwiedner)
Woody, D., Carpenter, J., & Scoville, N. 2000, in ASP Conf. Ser. 217, Imaging at Radio through Submillimeter Wavelengths, ed. J. G. Mangum & S. J. E. Radford (San Francisco: ASP), 317